Electronic Supplementary Information

The Effect of Polymer End-group on the Formation of Styrene – Maleic Acid Lipid Particles (SMALPs)

*George M. Neville,[a,b] Kerrie A. Morrison,[a,c] Ella Shilliday,[b] James Doutch,[d] Robert Dalgliesh,[d] Gareth J. Price [b,e] and Karen J. Edler *[c]‡*

1.0 Polymer Synthesis & Characterisation

1.1 RAFT Polymerisation of SMAnh

In accordance with the protocol adapted from Harrison and Wooley,[1] the monomers, styrene and maleic anhydride, the initiator, AIBN, and the RAFT agent, DDMAT, were dissolved in 1,4-dioxane in the molar ratios found in Table S1.

Table S1 Molar ratios used to synthesise the 2:1 styrene-maleic anhydride copolymer SMAnh-SC_{12}.

Reagent	Mr / $gmol^{-1}$	Mass / g	Mol	Predicted M_n / kDa[a]
Styrene	104.15	7.0021	0.0672	
MAnh	98.06	2.8273	0.0288	
1,4-Dioxane	88.11	21.000	0.2383	6
AIBN	164.21	0.3031	0.0018	
DDMAT	364.63	0.6335	0.0017	

[a] $Mn(pre) = (\frac{mol(styrne)\times Mr(styrne)\times conversion}{mol(DDMAT)}) + (\frac{mol(MAnh)\times Mr(MAnh)\times conversion}{mol(DDMAT)}) + Mr(DDMAT)$, where conversion is assumed to be 100%.

Reaction mixtures were sealed in a round bottomed flask before degassing with nitrogen and three subsequent freeze-thaw cycles, under vacuum, to purge oxygen that could potentially poison the initiator species and affect the resultant molecular weight. The flask was covered with foil to exclude light, before heating to 60 °C for 24 hours. Polymers were precipitated in 500 ml diethyl ether at 0 °C. For d-SMAnh, the procedure was identical, except for the substitution of appropriate masses of d_6-styrene for styrene. *E.g.* 7.40482 g d6-styrene.

1.2 End Group Modification of SMAnh-SC_{12} to SMAnh-CN

RAFT polymerisations results in a polymer end group dependent on the RAFT agent used. Here, this is dodecylthiocarbonothioylthio which is hydrophobic. A method for exchanging this end group for a hydrophilic cyanoisoproypyl group was adapted from the work of Chen *et al.*.[3] Scheme S1 highlights how the presence of excess radical initiators can cleave the end group without propagation of dead chains.

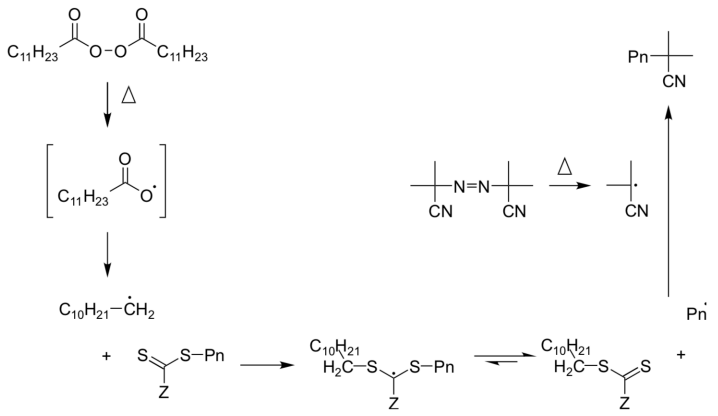

Scheme. S1 Reaction scheme for end group exchange from thiocarbonylthio to cyanoisopropyl.

1.3 Hydrolysis of SMAnh to SMA

Conversion of SMAnh to SMA was monitored using FTIR. As seen in Fig. S1, evidence of the transformation of MAnh to MA is primarily observed from the loss of anhydride peaks (~ 1854 cm^{-1}, 1773 cm^{-1}, 1220 cm^{-1}, 1075 cm^{-1} and 920 cm^{-1} etc.) and growth of acid peaks (~ 1563 cm^{-1}). Those peaks relating to styrene (~ 1453-1493 and 699-760 cm^{-1} etc.) are retained after reaction. Peaks arising from undetermined species generated during end group conversion to SMAnh-CN are seen to be purified out post hydrolysis to the acid form.

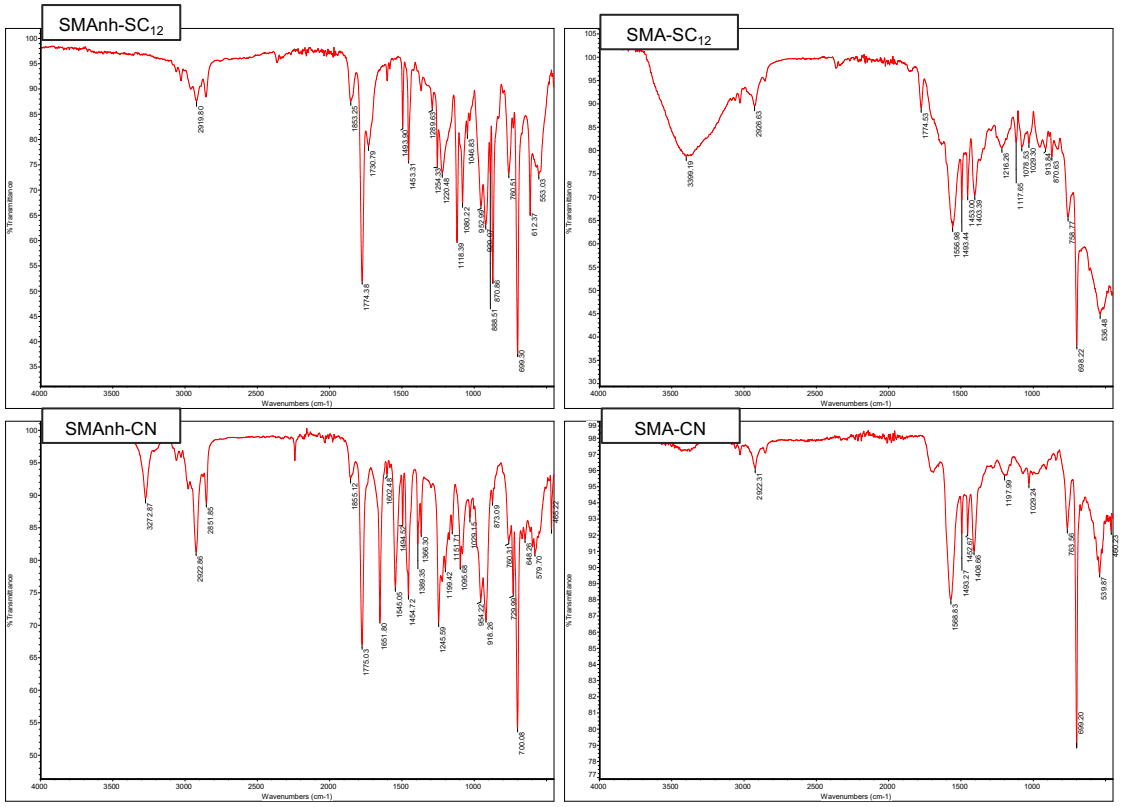

Fig. S1 FTIR spectra for SMAnh-SC_{12} and SMAnh-CN (left) before and (right) after hydrolysis to SMA.

1.4 ^{1}H & ^{13}C NMR Spectroscopy

In ^{1}H spectra for SMAnh copolymers (Fig. S2), the integral of the styrenic peak, *a*, compared to that of maleic anhydride, *b*, gives the 2:1 comonomer ratio when dived by the number of corresponding protons, 5 and 2, respectively. Thiocarbonylthio end groups afforded by RAFT at δ = 0.8,[5] are also identifiable and are preserved during hydrolysis.

^{13}C NMR was used to observe the introduction of a Sty-*alt*-MA-*homo*-Sty architecture, introduced by RAFT synthesis. It has been previously identified that peaks at 36.3 and 40.5 ppm refer to the alternating block, and those at 42.0 and 51.8 ppm, the styrene homoblock.[6] As seen in Fig. S3, SMAnh-SC_{12} contains this structure. Whilst SMAnh 2000 contains similar peaks, these are comparatively broadened, and the spectrum completely lacks the alternating peak at 36.3 ppm. Moreover, SMAnh-SC_{12} lacks the peak at 38.1 ppm, found in SMAnh 2000, representing semi-alternating, randomised structure.

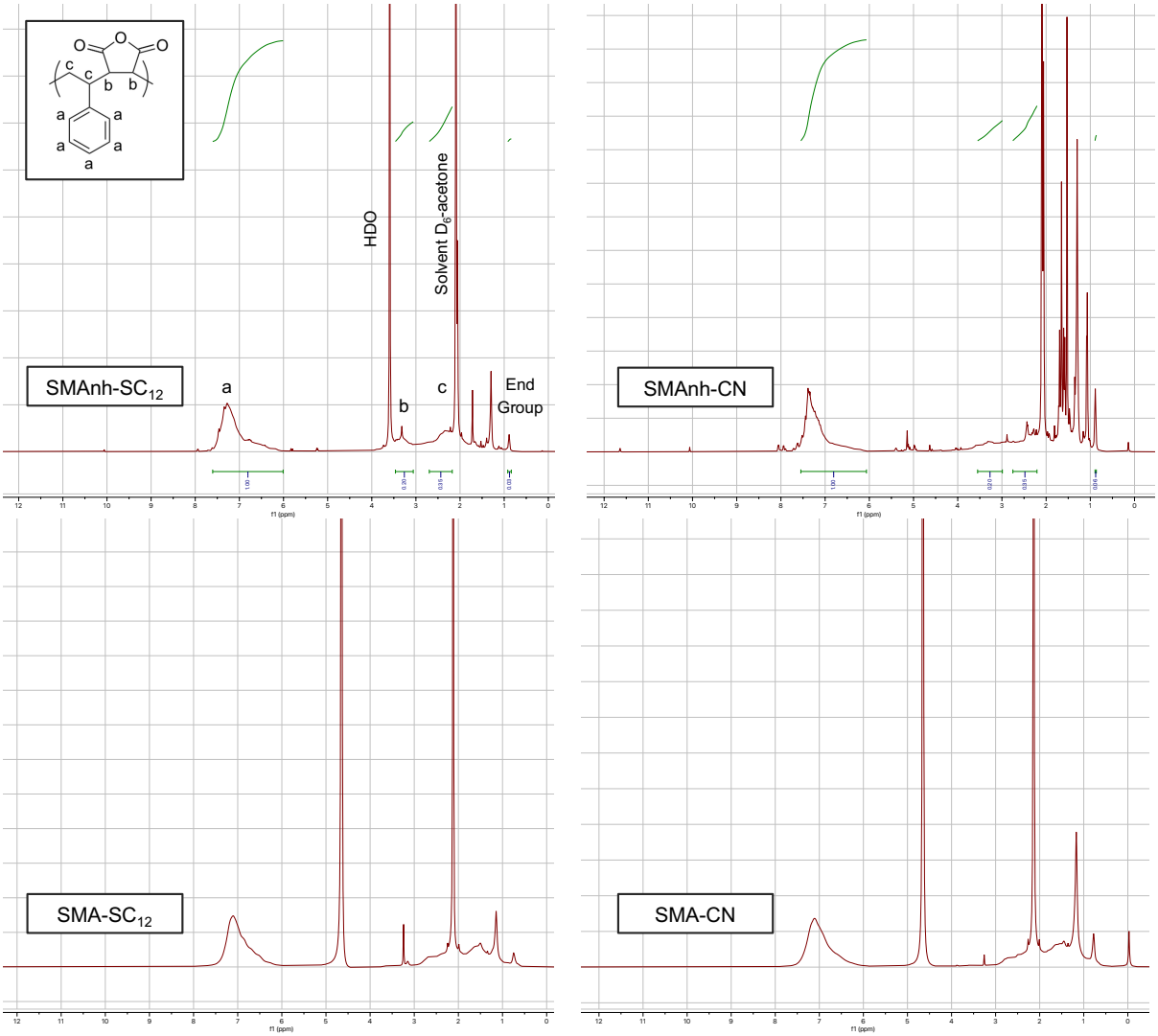

Fig. S2 ^{1}H NMR spectrum of (left) SMAnh-SC_{12} and (right) SMAnh-CN: (d_6-acetone): δ 7.60-6.05 (5H, broad, H_a), 3.05-3.50 (2H, broad, H_b), 2.3-2.70 (2H, broad H_c), 0.87-0.90 (3H, t, DDMAT end group).

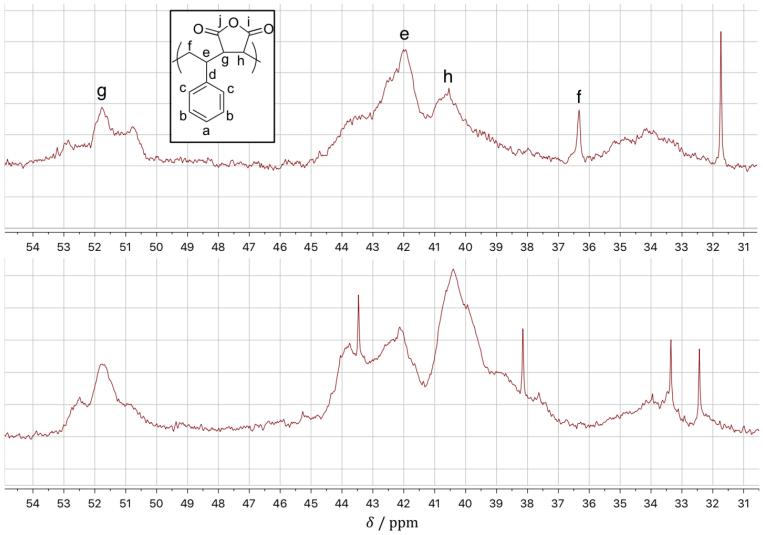

Fig. S3 ^{13}C NMR spectra of (top) SMAnh-SC_{12} and (bottom) SMAnh 2000 highlight polymer topology.

1.5 ^{1}H-^{15}N Heteronuclear Multiple Bond Correlation (HMBC) NMR

Experiments were conducted on a 500MHz *Bruker AV III HD* spectrometer, equipped with a liquid nitrogen cooled *Prodigy BBO* cryoprobe, operating at 500.2 MHz for ^{1}H spectra, and 50.7 MHz for ^{15}N spectra. Spectra were recorded at room temperature using 192 gradient increments, each containing 192 scans, taking 20.5 hours. Experiments were optimised for a ^{1}H-^{15}N coupling of 3 Hz.

HMBC NMR was used in an attempt to confirm the presence of non-hydrolysed nitrile groups in SMA-CN. The spectra (Fig. S4) show that both anhydride copolymers contain two nitrogen peaks at approximately ^{1}H 1.0 - 1.5 ppm (^{15}N 100 – 150 ppm). These likely relate to small molecules free in solution, such as unreacted AIBN radicals, as they do not correspond to polymeric peaks and had singlet structure. SMAnh-CN has two additional peaks at approximately ^{15}N 125 ppm, plausibly representing a nitrile, attached to styrene polymer units (^{1}H 7.5 – 6.0 ppm). Post hydrolysis, however, these peaks are no longer present. SMA-CN, does however, contain an additional peak (^{15}N 50 ppm) in comparison to SMA-SC_{12}, which has none. This peak is most likely an amine, although could feasibly represent a nitrile. Therefore, the results of these experiments are inconclusive as to whether the proposed cyanoisopropyl group survives hydrolysis, but does point to the preservation of some form of nitrogen environment. Caution must be taken when interpreting these results, as the sensitivities used were uncommonly high in order to detect nitrogen atoms that are expected to be at least four bonds away from the nearest hydrogen nucleus.

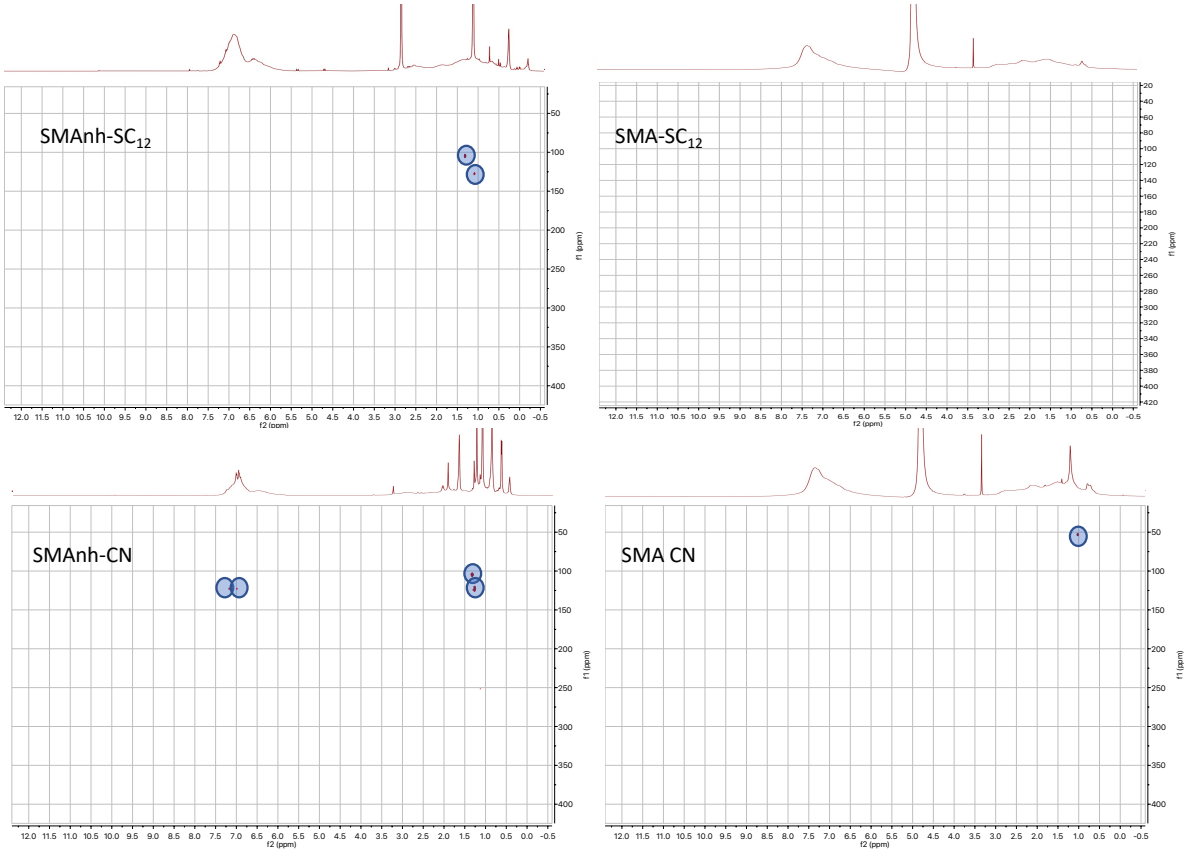

Fig. S4 ^{1}H-^{15}N HMBC spectra for anhydride polymers (left) and acid polymers (rights) for (top) SMA/nh-SC12 and (bottom) SMA/nh-CN.

2.0 Solution Behaviour and Neutron Scattering

2.1 Pendant Drop Tensiometry

Samples containing SMA polymers in solution at relevant concentrations in PBS were passed through needles to produce a small hanging droplet which was imaged at a typical rate of 10 images per second for 10 seconds to ensure a good average measurement (Fig. S5a). An iterative convergence calculation is then used to fit the shape of the drop to Equation S1, where γ is surface tension, $\Delta\rho$ is the difference in density of the light and heavy phase (Table S2), g is gravitational acceleration, D_e is the maximum diameter (Fig. S5b), and H is a correction coefficient between the horizontal and vertical D_e values:

$$\gamma = \frac{\Delta\rho g D_e^2}{H} \quad \text{(S1)}$$

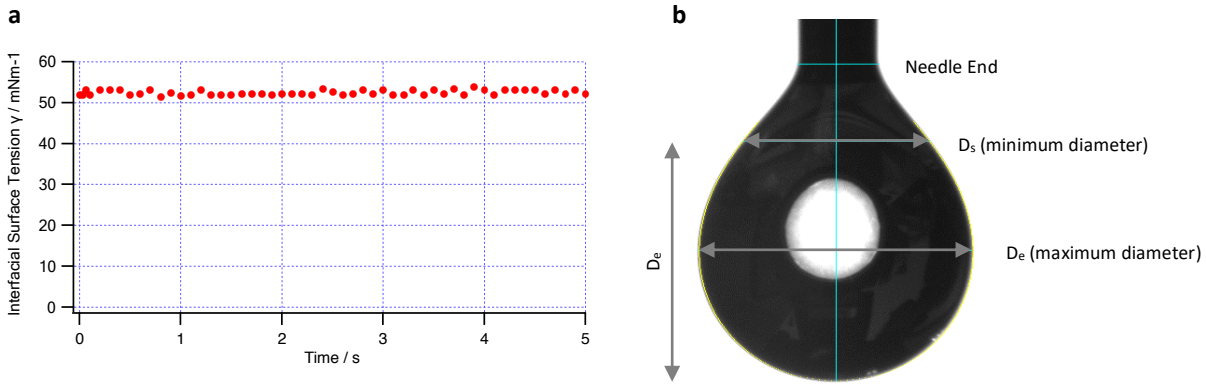

Fig. S5 (a) Plot of interfacial surface tension against time from *FTA 32* software. (b) Single image from *FTA 32* software where droplet shape has been outlined and divided into sections including needle end, D_s, and D_e.

Table S2 Densities of light and heavy phase used in calculation for respective interfacial surface tension measurements

Experiment	Phase	Density ρ / g cm^{-3}
Air-PBS	Air (Light)	0.0011
	PBS (Heavy)	1.0000
Dodecane-PBS	Dodecane (Light)	0.7500
	PBS (Heavy)	1.0000

2.3 Dynamic Light Scattering (DLS)

2.3.1 Zeta Potential

Table S3 Polymer aggregate and SMALP nanodisc zeta potentials from DLS.

Sample	Zeta Potential / mV
SMA-SC_{12} Aggregate (1.2% wt/v)	-24.7 ± 1.9
SMA-CN Aggregate (1.2% wt/v)	-24.8 ± 1.3
SMA 2000 Aggregate (1.2% wt/v)	-24.9 ± 1.9
SMA-SC_{12} Nanodisc	-18.0 ± 0.3
SMA-CN Nanodisc	-20.2 ± 0.5
SMA 2000 Nanodisc	-12.9 ± 1.2

2.3.2 Copolymer Aggregate Size

Table S4 Aggregate diameter and PDI from DLS measurements.

Aggregate Sample	Concentration / %(wt/v)	Temperature / °C	Diameter / nm[a]	PDI[a]
SMA-SC_{12}	0.02	25	10.24 ± 3.89	0.52 ± 0.18
SMA-SC_{12}	0.02	45	9.81 ± 0.92	0.28 ± 0.15
SMA-SC_{12}	0.02	65	10.78 ± 1.53	0.25 ± 0.05
SMA-CN	0.02	25	0.71 ± 0.04	0.66 ± 0.12
SMA-CN	0.02	45	2.14 ± 1.90	0.67 ± 0.17
SMA-CN	0.02	65	0.77 ± 0.03	0.93 ± 0.07
SMA 2000	0.02	25	2.01 ± 0.82	0.43 ± 0.04
SMA 2000	0.02	45	2.69 ± 0.94	0.28 ± 0.12
SMA 2000	0.02	65	1.45 ± 0.68	0.59 ± 0.23
SMA-SC_{12}	0.10	25	13.14 ± 0.20	0.14 ± 0.01
SMA-SC_{12}	0.10	45	12.07 ± 0.38	0.13 ± 0.02
SMA-SC_{12}	0.10	65	12.23 ± 0.20	0.14 ± 0.01
SMA-CN	0.10	25	13.16 ± 0.54	0.54 ± 0.01
SMA-CN	0.10	45	13.04 ± 0.75	0.56 ± 0.01
SMA-CN	0.10	65	12.85 ± 0.69	0.52 ± 0.01
SMA 2000	0.10	25	2.56 ± 0.02	0.18 ± 0.02
SMA 2000	0.10	45	3.31 ± 0.23	0.30 ± 0.01
SMA 2000	0.10	65	2.06 ± 0.02	0.39 ± 0.09

[a] Error reported at 95% C.I. from average of 5 sets of at least 12 scans.

2.3.3 SMALP Nanodisc Sizes from DLS measurements

Table S5 SMALP nanodisc diameters and PDI.

Nanodisc Sample	Lipid Species	Temperature / °C	Diameter / nm[a]	PDI[a]
SMA-SC_{12}	DMPC	25	18.9 ± 1.0	0.48 ± 0.01
SMA-SC_{12}	DMPC	45	12.8 ± 1.0	0.26 ± 0.01
SMA-SC_{12}	DMPC	65	11.2 ± 1.6	0.25 ± 0.01
SMA-CN	DMPC	25	14.86 ± 0.24	0.45 ± 0.01
SMA-CN	DMPC	45	14.14 ± 0.15	0.45 ± 0.01
SMA-CN	DMPC	65	12.74 ± 0.44	0.44 ± 0.01
SMA 2000	DMPC	25	5.92 ± 0.11	0.27 ± 0.02
SMA 2000	DMPC	45	5.37 ± 0.14	0.23 ± 0.06
SMA 2000	DMPC	65	4.91 ± 0.19	0.19 ± 0.05
SMA-SC_{12}	DMPC+gramicidin	25	22.48 ± 0.31	0.25 ± 0.01
SMA-CN	DMPC+gramicidin	25	30.43 ± 0.96	0.25 ± 0.01
SMA 2000	DMPC+gramicidin	25	5.86 ± 0.17	0.50 ± 0.01
SMA-SC_{12}	DPPC	25	88.00 ± 38	0.24 ± 0.01
SMA-CN	DPPC	25	16.99 ± 0.27	0.23 ± 0.01
SMA 2000	DPPC	25	9.78 ± 0.30	0.14 ± 0.01
SMA-SC_{12} (B)	DMPC	25	18.69 ± 0.13	0.17 ± 0.01
SMA-SC_{12} (C)	DMPC	25	20.71 ± 0.82	0.18 ± 0.01
SMA-CN (B)	DMPC	25	16.34 ± 0.72	0.61 ± 0.02
SMA-CN (C)	DMPC	25	15.75 ± 0.61	0.58 ± 0.01

[a] Error reported at 95% C.I. from average of 5 sets of at least 12 scans.

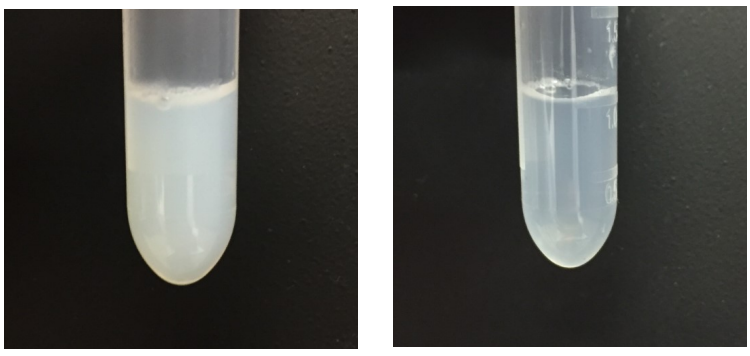

Fig. S6 Images of DPPC solutions at least 24 hours after addition of (left) SMA-SC_{12} and (right) SMA-CN, highlighting the apparent inability of SMA-SC_{12} to solubilise DPPC.

2.4 SANS

SANS was performed at the *ISIS Neutron and Muon Source* (Rutherford Appleton Laboratory, Didcot, UK), on the *Larmor* and *Zoom* instruments (doi:10.5286/ISIS.E.RB1910182), using 1 mm quartz *Hellma* cells at 25 °C.

SANS data were reduced with background subtraction using *Mantid* software[8] before the varying sample contrasts were simultaneously fitted using the *NIST* SANS analysis package within *Igor Pro.*[9] Copolymer aggregates were fitted to either core shell spherical (Fig. S7a) or cylindrical models (Fig. S7b) within the package.[10] These describe either spherical or cylindrical forms with a shell of uniform thickness over the entire particle. Core SLDs were held constant as those calculated for Sty (see Table S6), whereas the shell started with the SLD calculated from a 1:1 Sty:MA composition and then fitted to find the percentage hydration. Radial polydispersity was also accounted for in the model, where values were aligned to those found by DLS.

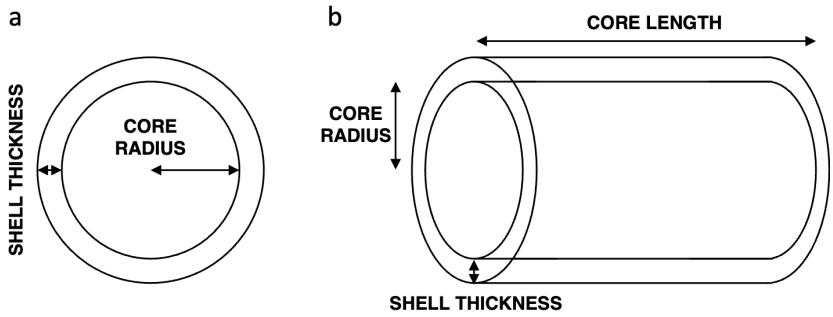

Fig. S7 Cross section schematic of core shell (a) spherical and (b) cylindrical models used to fit SANS data.

Scattering patterns from SMALP solutions were fitted using a version of the core shell bicelle model, adapted to include the percentage polymer in the core and solvent in the rim as separate parameters (Fig. 1b. in the main article). The face thickness and face hydration of the nanodiscs were set to values found from DMPC head groups (Table S6).[7]

Table S6 Model parameters held during fitting. Structural components of aggregates defined as in Fig. S7. Structural components of SMALPs defined as in Fig. 1a (main text).

Parameter	Held Value
SLD Aggregate Styrene Core (C_8H_8)	1.439×10^{-6} Å^{-2}
SLD Aggregate Shell (1:1 Sty:MA)	1.818×10^{-6} Å^{-2}
SLD Aggregate Styrene Core (C_8D_8)	6.121×10^{-6} Å^{-2}
SLD Aggregate Shell (1:1 dSty:MA)	4.116×10^{-6} Å^{-2}
SLD SMALP rim (2:1 Sty:MA)	1.696×10^{-6} Å^{-2}
SLD SMALP rim (2:1 dSty:MA)	$4..779\times10^{-6}$ Å^{-2}
SLD SMALP Face	1.84×10^{-6} Å^{-2}
Hydration SMALP Face[a]	57%
Thickness SMALP Face[a]	0.8 nm
SLD hDMPC SMALP Core	-0.5×10^{-6} Å^{-2}
SLD dDMPC SMALP Core	5.6×10^{-6} Å^{-2}
SLD 100% D_2O Solvent	6.35×10^{-6} Å^{-2}
SLD 70% D_2O Solvent	4.277×10^{-6} Å^{-2}
SLD 50% D_2O Solvent	2.895×10^{-6} Å^{-2}
Charge	20 mV
Monovalent Salt Concentration	0.25 M
Temperature	298 K
Dielectric Constant	78

[a] From ref [7].

2.4.1 Copolymer Aggregates

SMA-SC_{12} aggregates were fitted to a core shell sphere model with a polydisperse radius, whereas SMA-CN aggregates were better fitted to a core shell cylinder model with polydisperse radius and length. Fitting parameters for SMA-SC_{12} and SMA-CN aggregates are found in Table S7 and Table S8 respectively. Additionally, SMA-CN aggregates fitted to a core shell sphere model are presented in Fig. S8 Table S9 to highlight the unsatisfactory fit.

Table S7 Fitting parameters for SMA-SC_{12} spherical aggregates.

Parameter	Held Value
Core Radius [nm]	3 (± 1)
Radial Polydispersity	0.28 (±0.03)
Shell Thickness [nm]	1.1 (± 0.4)
Hydration Shell [%]	40 (± 10)

Table S8 Fitting parameters for SMA-CN cylindrical aggregates.

Parameter	Fit Value
Core Radius [nm]	3 (± 1)
Core Length [nm]	1.5 (± 0.4)
Radial Polydispersity	0.56 (±0.03)
Shell Thickness [nm]	1.5 (± 0.4)
Hydration Shell [%]	15 (± 10)

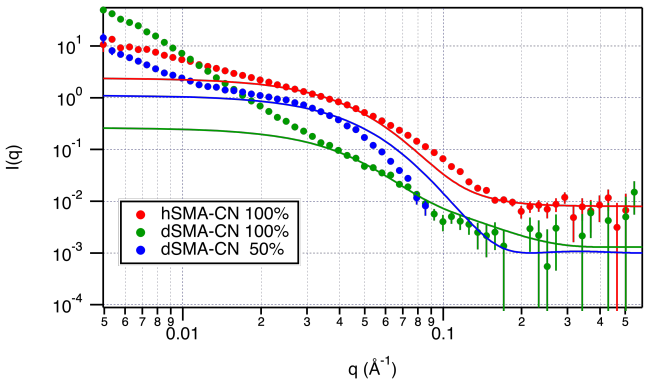

Fig. S8 SANS data for SMA-CN aggregates fitted to a polydisperse core shell sphere model, highlighting the poorer fit achieved compared to a core shell cylinder model.

Table S9 Fitting parameters for SMA-CN fit as spherical aggregates, highlighting the comparatively poorer fit achieved.

Parameter	Fit Value
Core Radius [nm]	2 (± 1)
Radial Polydispersity	0.56 (±0.07)
Shell Thickness [nm]	1.5 (± 0.3)
Hydration Shell [%]	15 (± 10)

2.4.2 SMALP Nanodiscs

Here, all data was fitted using a SMALP model based on a core shell bicelle model in the NIST SANS Analysis package in Igor Pro (Fig. 1b. main text). Fitted parameter values for nanodiscs from SMA-SC_{12} and SMA-CN can be found in Tables S10-S11 and Fig. S10a; and Tables S12-S13 and Fig. S10b, respectively. Data sets from the hydrogenated and deuterated polymers have been fitted separately as the model directly incorporates the SLD of the polymer. Data relating to SMA-SC_{12} (B) and(C) can be found in Table S14-S15 and Fig. S10 and those to SMA-CN (B) and (C) in Table S16-17 and Fig. S11.

Table S10 Fitting parameters for hSMA-SC_{12} DMPC SMALPs.

Parameter	Fit Value
Mean Core Radius [nm]	3.4 (± 0.4)
Radial Polydispersity	0.29 (± 0.05)
Length [nm]	3 (± 0.3)
Rim Thickness [nm]	1.1 (± 0.4)
Polymer in Core [%]	31 (± 6)
Hydration Rim [%]	29 (± 4)

Table S11 Fitting parameters for dSMA-SC_{12} DMPC SMALPs.

Parameter	Fit Value
Mean Core Radius [nm]	4.4 (± 0.6)
Radial Polydispersity	0.20 (± 0.03)
Length [nm]	2.9 (± 0.2)
Rim Thickness [nm]	1.1 (± 0.2)
Polymer in Core [%]	26 (± 3)
Hydration Rim [%]	33 (± 4)

Table S12 Fitting parameters for hSMA-CN DMPC SMALPs.

Parameter	Fit Value
Mean Core Radius [nm]	3.8 (± 0.3)
Radial Polydispersity	0.33 (± 0.04)
Length [nm]	3.4 (± 0.3)
Rim Thickness [nm]	0.9 (± 0.3)
Polymer in Core [%]	24 (± 6)
Hydration Rim [%]	32 (± 4)

Table S13 Fitting parameters for dSMA-CN DMPC SMALPs.

Parameter	Fit Value
Mean Core Radius [nm]	4.1 (± 0.4)
Radial Polydispersity	0.46 (± 0.07)
Length [nm]	3.3 (± 0.3)
Rim Thickness [nm]	1.0 (± 0.3)
Polymer in Core [%]	20 (± 4)
Hydration Rim [%]	30 (± 4)

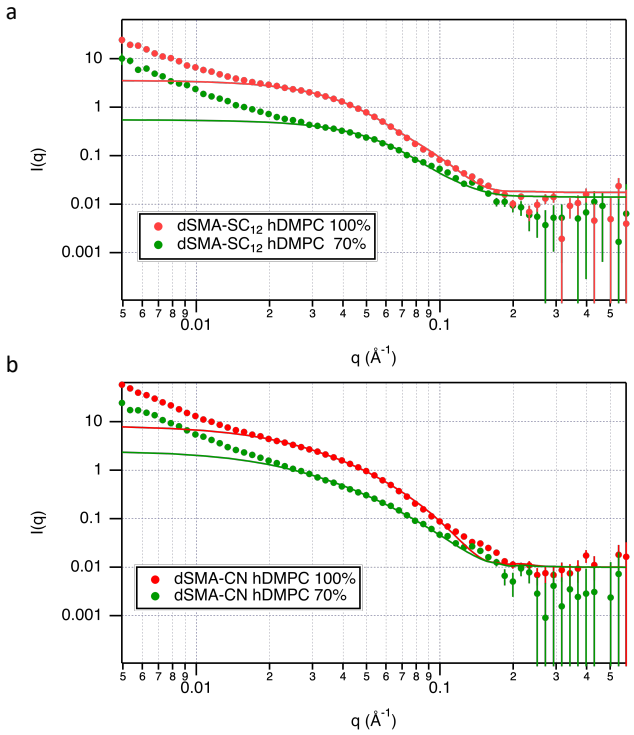

Fig. S9 SANS data for (a) dSMA-SC_{12} and (b) dSMA-CN nanodiscs with hDMPC at various contrasts fit to a SMALP model based on the core shell bicelle model.

Table S14 Fitting parameters for hSMA-SC_{12} (B) DMPC SMALPs.

Parameter	Fit Value
Mean Core Radius [nm]	4.5 (± 0.5)
Radial Polydispersity	0.26 (± 0.04)
Length [nm]	3.3 (± 0.3)
Rim Thickness [nm]	0.9 (± 0.4)
Polymer in Core [%]	26 (± 7)
Hydration Rim [%]	30 (± 5)

Table S15 Fitting parameters for hSMA-SC_{12} (C) DMPC SMALPs.

Parameter	Fit Value
Mean Core Radius [nm]	4.9 (± 0.6)
Radial Polydispersity	0.31 (± 0 .04)
Length [nm]	3.8 (± 0.2)
Rim Thickness [nm]	0.8 (± 0.4)
Polymer in Core [%]	35 (± 6)
Hydration Rim [%]	25 (± 5)

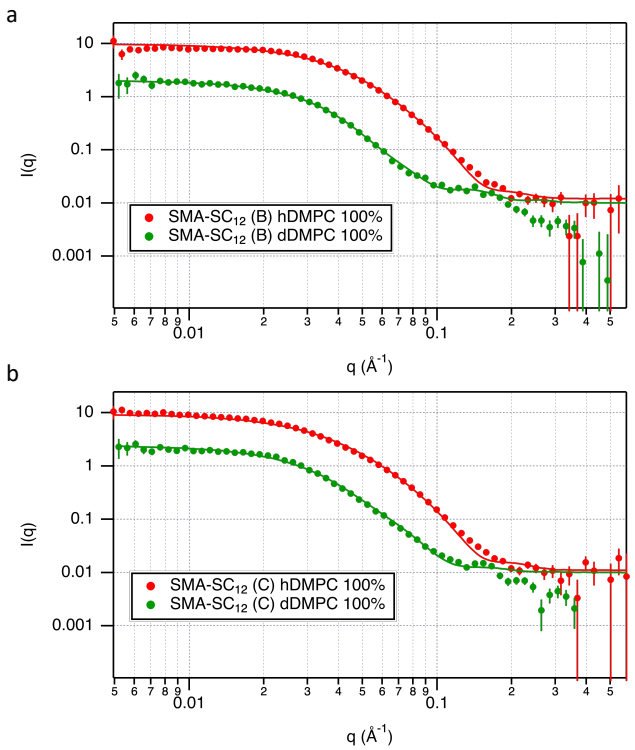

Fig. S10 SANS data for (a) SMA-SC_{12} (B) and (b) SMA-SC_{12} (C) nanodiscs with hDMPC and dDMPC at 100% D_2O contrast fit to in-house SMALP model based on core shell bicelle..

Table S16 Fitting parameters for hSMA-CN (B) DMPC SMALPs.

Parameter	Fit Value
Mean Core Radius [nm]	4.0 (± 0.6)
Radial Polydispersity	0.36 (± 0.04)
Length [nm]	3.2 (± 0.4)
Rim Thickness [nm]	1.0 (± 0.2)
Polymer in Core [%]	20 (± 8)
Hydration Rim [%]	30 (± 8)

Table S17 Fitting parameters for hSMA-CN (C) DMPC SMALPs.

Parameter	Fit Value
Mean Core Radius [nm]	3.7 (± 0.4)
Radial Polydispersity	0.35 (± 0.03)
Length [nm]	2.9 (± 0.2)
Rim Thickness [nm]	1.1 (± 0.2)
Polymer in Core [%]	21 (± 6)
Hydration Rim [%]	30 (± 6)

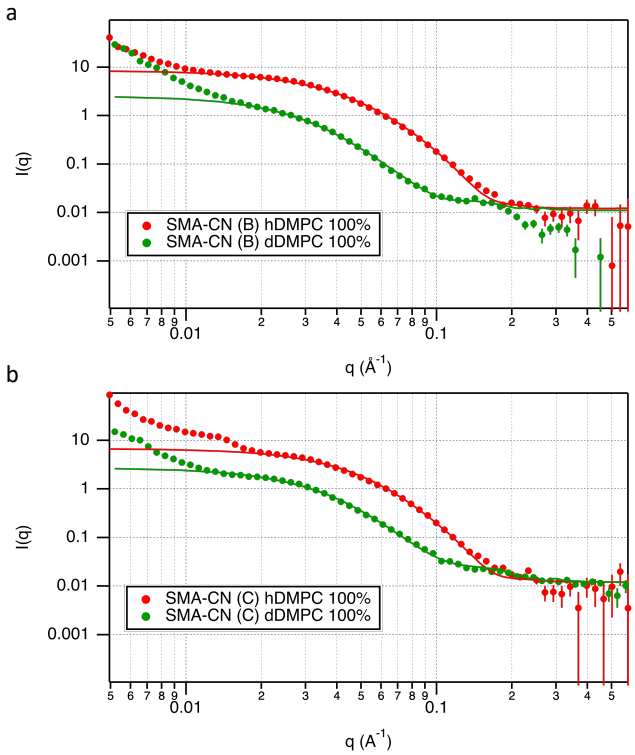

Fig. S11 SANS data for (a) SMA-CN (B) and (b) SMA-CN (C) nanodiscs with hDMPC and dDMPC at 100% D_2O contrast fit to a SMALP model based on core shell bicelle.

3.0 References

1. S. Harrisson and K. L. Wooley, *Chem. Commun.*, 2005, 26, 3259–3261.
2. S. C. Hall, C. Tognoloni, G. J. Price, B. Klumperman, K. J. Edler, T. R. Dafforn and T. Arnold, *Biomacromolecules*, 2018, 19, 761-772.
3. M. Chen, G. Moad and E. Rizzardo, *J. Polym. Sci. Part A: Polym. Chem.*, 2009, **47**, 6704–6714.
4. A. F. Craig, E. E. Clark, I. D. Sahu, R. Zhang, N. D. Frantz, M. S. Al-Abdul-Wahid, C. Dabney-Smith, D. Konkolewicz and G. A. Lorigan, *Biochimica et Biophysica Acta (BBA)-Biomembranes*, 2016, 1858, 2931–2939.
5. O. O. Oyeneye, W. Z. Xu and P. A. Charpentier, *RSC Adv.*, 2015, **5**, 76919-76926.
6. P. F. Barron, D. J. T. Hill, J. H. O'Donnell and P. W. O'Sullivan, *Macromolecules*, 1984, **17**, 1967-1972.
7. M. B. Smith, D. J. McGillivray, J. Genzer, M. Lösche and P. K. Kilpatrick, *Soft Matter*, 2010, **6**, 862–865.
8. O. Arnold, J. C. Bilheux, J. M. Borreguero, A. Buts, S. I. Campbell, L. Chapon, M. Doucet, N. Draper, R. Ferraz Leal, M. A. Gigg, V. E. Lynch, A. Markvardsen, D. J. Mikkelson, R. L. Mikkelson, R. Miller, K. Palmen, P. Parker, G. Passos, T. G. Perring, P. F. Peterson, S. Ren, M. A. Reuter, A. T. Savici, J. W. Taylor, R. J. Taylor, R. Tolchenov, W. Zhou and J. Zikovsky, *Nucl. Instrum. Methods Phys. Res. A: Accel. Spectrom. Detect. Assoc. Equip.*, 2014, **764**, 156-166.
9. S. R. Kline, *J. Appl. Crystallogr.*, 2006, **39**, 895-900.
10. A. Guinier, G. Fournet, Small-angle scattering of X-rays. John Wiley and Sons, New York, 1955.